J Sol-Gel Sci Techn (2007) 42:13–20
DOI 10.1007/s10971-006-1518-2

A new study on the kinetics of Stöber synthesis by in-situ liquid ^{29}Si NMR

Yao Xu · Dong Wu · Yuhan Sun · Hongchang Gao · Hanzhen Yuan · Feng Deng

Received: 9 February 2006 / Accepted: 10 October 2006 / Published online: 1 February 2007

Abstract Liquid-state ^{29}Si NMR was used to investigate the hydrolysis and condensation kinetics of ammonia-catalyzed tetraethoxysilane (TEOS) in methanol system. The reactive rate constants were calculated by applying first-order reaction approximation and the steady state approximation theory. The reaction orders with respect to TEOS, ammonia and water were derived, as well as the activation energies and the Arrhenius constants. It was found that the formation of intermediate species $Si(OH)(OEt)_3$ was the rate-limiting step and its reaction rate equation was $r_{TEOS} = 7.41 \times 10^{-3}[TEOS][NH_3]^{0.333}[H_2O]^{0.227}$. Higher reactive temperature benefited the hydrolysis of TEOS. The results presented here indicated quantificationally that the formation of colloidal SiO_2 particles was controlled by the initial hydrolysis of TEOS.

Keywords Stöber synthesis · Reaction kinetics · Nuclear magnetic resonance

1 Introduction

Monodisperse silica nanoparticles have been widely applied in the fields of optics, electronics, catalysis, sensor and biology [1]. **S**töber synthesis [2] was the first method to produce this kind of uniform silica nanoparticles through ammonia-catalyzed hydrolysis and condensation of ethoxysilanes in low molecule-weight alcohol. Thus-obtained spheric SiO_2 particles may have diameters ranged from 5 nm to 2000 nm. The understanding on the kinetic of **S**töber reaction is very helpful for the control of size and growth of SiO_2 particles. Deep and detailed kinetics of Stöber synthesis were not obtained by the previous researches [3–8], and there were some contradiction between different explanations. And the exact reaction orders haven't been derived till now. In detail, there were two different viewpoints about the rate-limiting step of Stöber reaction to form SiO_2 nucleus: the condensation of hydrolyzed monomer or the initial hydrolysis of TEOS. The work of Sadasivan [8] supported the first viewpoint, thinking a fully hydrolyzed dimmer $(HO)_3SiOSi(OH)_3$ was the key intermediate species. However, the second viewpoint was supported by Lee [3], Matsoukas [4], and Green [7] using light scattering, Raman spectroscopy, and liquid ^{29}Si NMR technologies. Out of above considerations, the present work aimed to a deep understanding of the hydrolysis and condensation kinetics of TEOS under ammonia-catalysis and then to determine what should be the true rate-limiting step of Stöber reaction. To our knowledge, the precise rate constants and reaction orders obtained here was the first time.

Y. Xu (✉) · D. Wu · Y. Sun
State Key Laboratory of Coal Conversion, Institute of Coal Chemistry, Chinese Academy of Sciences,
Taiyuan 030001, China
e-mail: xuyao@sxicc.ac.cn

H. Gao · H. Yuan · F. Deng
State Key Laboratory of Magnetic Resonance & Atomic & Molecular Physics, Wuhan Institute of Physics and Mathematics, Chinese Academy of Sciences,
Wuhan 430071, China

2 Experiment

Reagent grade ammonium hydroxide (26% NH_3), methanol, deionized and distilled water, and TEOS were used, and the preparation conditions of samples are presented in Table 1.

NMR sample was prepared by mixing two parts: solution A, TEOS was dissolved in half of the total methanol and stirred for 20 min; solution B, deionized water and aqueous ammonia hydroxide solution was dissolved into another half

Table 1 Reaction compositions

Sample	$TEOS/CH_3OH/H_2O/NH_3$	T/°C
(a)	1/12.5/4/0.18	25
(b)	1/12.5/4/0.18	35
(c)	1/12.5/4/0.18	45
(d)	1/12.5/4/0.045	25
(e)	1/12.5/4/0.36	25
(f)	1/12.5/2/0.18	25
(g)	1/12.5/6/0.18	25
(h)	1/12.5/8/0.18	25

of the total methanol and stirred for 5 min. The reaction was initiated by mixing solution A and B. After vigorous stirring of 5 min, the mixture of solutions A and B was transferred to an NMR sample tube (5 mm O. D.) and immediately analyzed. Chromium (III) acetyl acetonate ($Cr(acac)_3$, 1%) was added as the spin relaxation agent. Many studies [9, 10] have shown that $Cr(acac)_3$ had no effect on the studied reactions. All ^{29}Si NMR experiments were carried out in duplicate on a UNITY INOVA-500 Spectroscopy at a spectral frequency of 99.351 MHz. To achieve sufficient signal intensity, 168 scans were acquired for each spectrum with a 3 s pulse delay using a 90°pulse angle. During the experiments, gelation did not occur and the transesterification reaction can be ignored [7].

3 Results and discussion

3.1 ^{29}Si NMR spectra and data analysis

Liquid ^{29}Si NMR technology provides a very useful tool to obtain valuable information about the chemistry structures of silicon alkoxides and their hydrolyzed or condensed derivates [11, 12]. It allows identification and quantification of soluble Si-containing species in solution, thus enable kinetic data to be extracted. The disappearance of monomer, TEOS, from its initial level and the appearance of the intermediate species are presented by the typical ^{29}Si NMR spectra (samples a, c, d, and h) in Fig. 1. In order to assign the ^{29}Si NMR chemical shift for different soluble

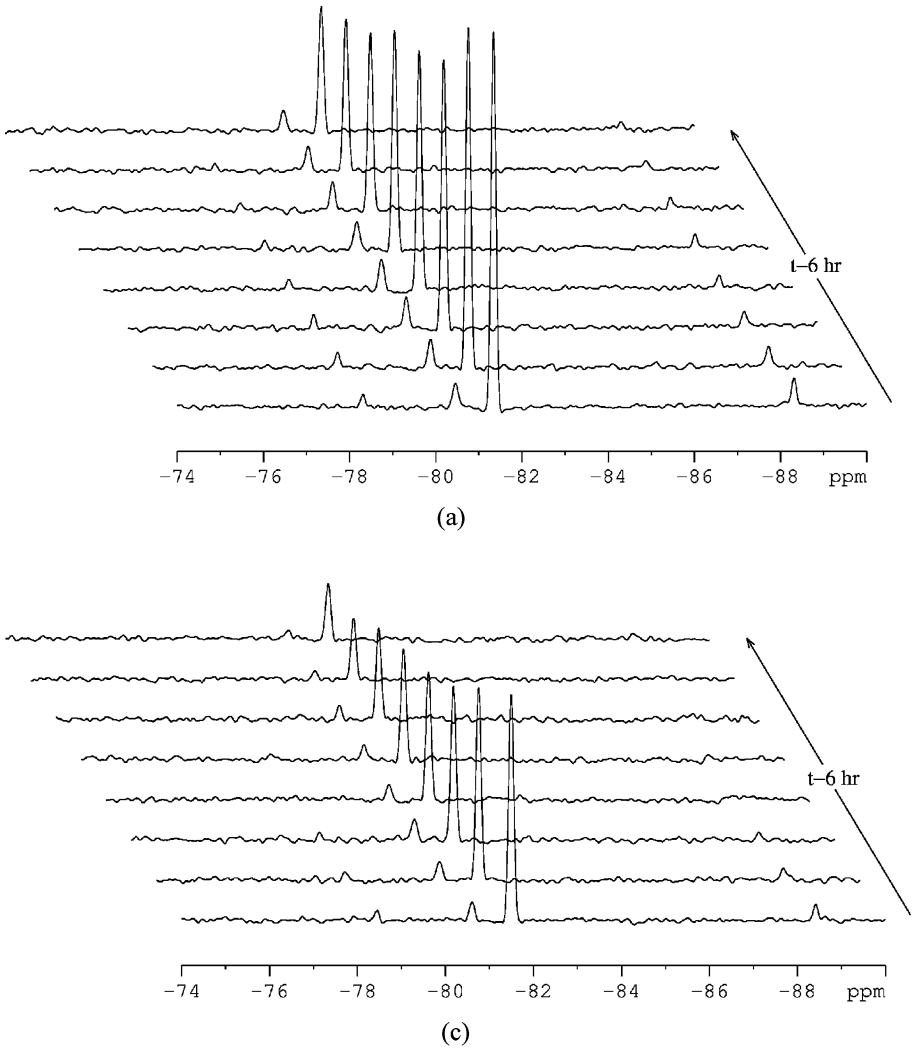

Fig. 1 The typical ^{29}Si NMR spectra of the solutions with ratio of $TEOS:CH_3OH:H_2O:NH_3$ at (a) 1:12.5:4:0.18 (25°C), (c) 1:12.5:4:0.18 (45°C), (d) 1/12.5/4/0.045 (25°C), (h) 1/12.5/8/0.18 (25°C)
(*Continued on next page*)

Fig. 1 (Continued)

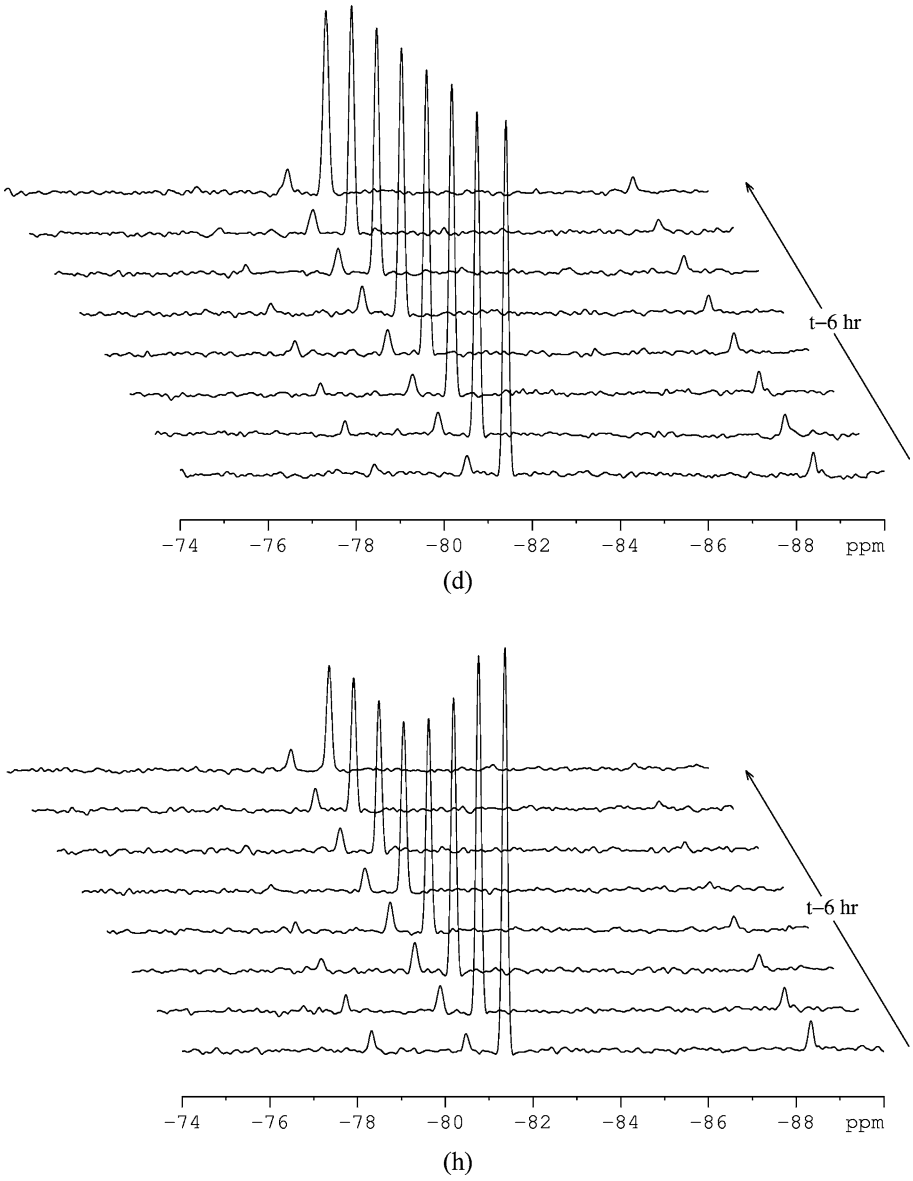

silicon species, the traditional notations were adapted [13]: Q presents the tetrafunctional silicon in TEOS. The symbol Q_m^n denotes the products of hydrolysis or condensation of TEOS, where m and n are the number of Si–O–Si bridges and the number of silanol groups surrounding Si atom respectively. The detailed chemical shift of each soluble Si species and the corresponding molecular structure are listed in Table 2. According to the studies of Lee [3] and Green [7], the chemical shift of TEOS is at –81.3 ppm; the resonance signals of two hydrolysis intermediate species, Q_0^1 and Q_0^3, appear at –80.4 ppm and –78.3 ppm respectively; the NMR peak at –88.3 ppm corresponds to the dimmer Q_1^0. The resonance of Q_0^2 is not observed probably because of the fast condensation of the intermediate Q_0^2 under basic conditions [7].

The relative concentrations of soluble intermediate Si species were determined by integrating the resonance peak

Table 2 ^{29}Si NMR chemical shift

	Structures	δ
Q_0^0	$Si^*(OEt)_4$	–81.3
Q_0^1	$Si^*(OEt)_3OH$	–80.4
Q_3^0	$Si^*(OEt)_2(OH)_2$	–
Q_0^3	$Si^*(OEt)(OH)_3$	–78.3
Q_1^0	$(EtO)_3Si^*OSi(EtO)_3$	–88.3

in NMR spectra. The integrated area of the initial Q_0^0 peak of TEOS before the addition of catalyst and water was taken as 100%. Shown in Fig. 2, the typical time-dependent concentration (samples a, c, d, and h) is the base of further calculation of the rate constants. In Fig. 2, the time-dependence of monomer concentration (Q_0^0) was obtained by fitting the experimental data with an exponential decay of first order. The time-dependences of the intermediate species

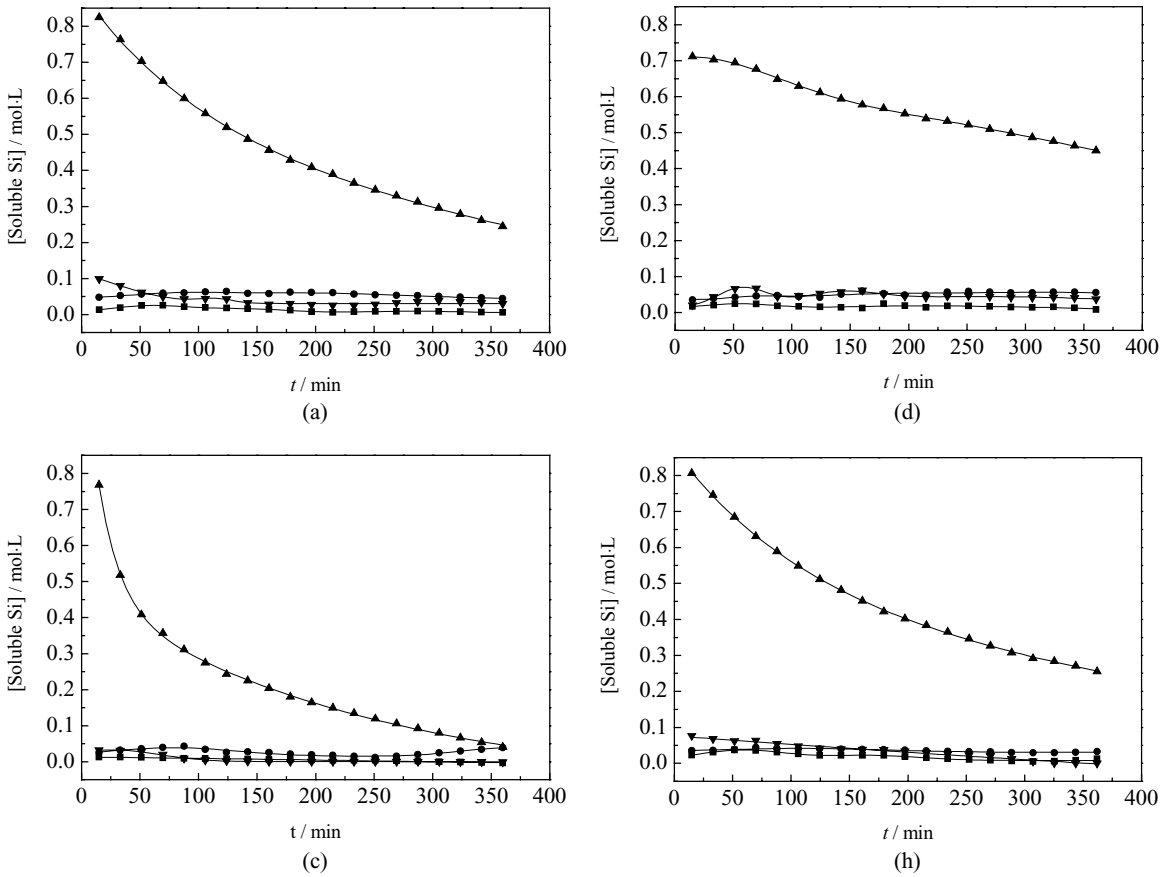

Fig. 2 The time-dependent concentrations of soluble Si species for the solutions with ratio of TEOS:CH_3OH:H_2O:NH_3 at (a) 1:12.5:4:0.18 (25°C), (c) 1:12.5:4:0.18 (45°C), (d) 1/12.5/4/0.045 (25°C), (h) 1/12.5/8/0.18 (25°C). ■ —Q_0^3; ● —Q_0^1; ▲ —Q_0^0; ▼ —Q_1^0

concentrations (Q_0^1, Q_0^3, Q_1^0) were obtained only to guide the eye. The effect of reaction temperature on the kinetics is obtained by comparing samples (a), (b) and (c). The effect of ammonia content on the kinetics is obtained by comparing samples (a), (d) and (e). The effect of water content on the kinetics is obtained by comparing samples (a), (f), (g) and (h). Therefore a qualitative conclusion can be easily drawn from Figs. 1 and 2: the hydrolysis of TEOS can be speeded up by increasing the ammonia content, water content, or reactive temperature.

3.2 Reaction kinetics of Stöber synthesis

The overall hydrolysis of TEOS can be described as equation:

$$\mathrm{Si(OEt)_4} + x\mathrm{H_2O} \longrightarrow (\mathrm{OH})_x\mathrm{Si(OEt)}_{4-x} + x\mathrm{EtOH}. \qquad (1)$$

In fact, the hydrolysis of precursor is a step-by-step process and it runs nearly simultaneously with the condensation that makes the reaction mechanism more complex. So based on this consideration, Harris [6] and Lee [3] suggested a detailed reaction model and a simple reaction model respectively. In fact it is impossible to calculate the exact rate constants according to the detailed model. So a simple hydrolysis and condensation model of TEOS is adopted here like follow according to Green's proposal [7].

$$Q_0^0 + \mathrm{H_2O} \xrightarrow{k_{\mathrm{h1}}} Q_0^1 + \mathrm{EtOH} \qquad (2)$$

$$Q_0^1 + 2\mathrm{H_2O} \xrightarrow{k_{\mathrm{h2}}} Q_0^3 + 2\mathrm{EtOH} \qquad (3)$$

$$2Q_0^3 \xrightarrow{k_c} \mathrm{SiO_2} + \mathrm{EtOH} + \mathrm{H_2O} \qquad (4)$$

where k_{h1}, k_{h2}, and k_{c} are the rate constants for Eqs. (2)–(4), respectively. In fact, Q_0^3 species can condense with each other to form Q_1^4 like Eq. (4), but Q_1^4 can't be detected in experiments, so this reaction isn't taken into account here. Considering that the condensation species can be easily detected even for those species larger than Q_1^4, the invisibility of Q_1^4 may be due to the very low concentration of it in tested solution. In this case, there must be a fast exhaustion of Q_1^4 that make its concentration lower than the NMR detective limit. The most possible reason for this exhaustion is because Q_1^4 quickly participate in the further nucleation and disappear in the "eye" of NMR instrument.

To obtain the reaction orders of the hydrolysis and condensation of TEOS, the concentrations of the starting reactants were varied. The rate equation for the reaction (2) is as follows

$$r_{\mathrm{TEOS}} = d\left[\mathrm{Q}_0^0\right]/\mathrm{dt} = k_{\mathrm{h1}}\left[\mathrm{Q}_0^0\right]^{\alpha}[\mathrm{NH_3}]^{\beta}[\mathrm{H_2O}]^{\gamma}, \quad (5)$$

where the exponents α, β and γ are the reaction orders belonging to TEOS, NH_3 and H_2O respectively. Since NH_3 is used as the catalyst during the hydrolysis and the condensation, its concentration can be considered constant. The change of water content was less than 5% of the initial level [14], so it is also considered invariable. If we define

$$k'_{\mathrm{h}} = k_{\mathrm{h1}}[\mathrm{NH_3}]^{\beta}[\mathrm{H_2O}]^{\gamma}, \quad (6)$$

the rate Eq. (5) can be simplified to

$$r_{\mathrm{TEOS}} = d\left[Q_0^0\right]/dt = k'_{\mathrm{h}}\left[Q_0^0\right]^{\alpha} \quad (7)$$

As can be seen in Fig. 2, the exponentially fitted time-dependent concentration of Q_0^0 is a good approximation for the experimental data. In this case, it is assumed that the reaction (2) is of first-order, i.e., $\alpha = 1$, so the integration of Eq. (7) leads to

$$\ln\left[Q_0^0\right] = \ln\left[Q_0^0\right]_0 - k'_h t \quad (8)$$

Thus a plot of $\ln[Q_0^0]$ vs. t should yield a straight line with $-k'_{\mathrm{h}}$ as slope and $\ln[Q_0^0]_0$ as intercept, which are shown in Fig. 3. This good linearity proves $\alpha = 1$ indeed. Furthermore, taking the logarithm of Eq. (6) will give

$$\ln k'_{\mathrm{h}} = \ln k_{\mathrm{h1}} + \beta \ln[\mathrm{NH_3}] + \gamma \ln[\mathrm{H_2O}] \quad (9)$$

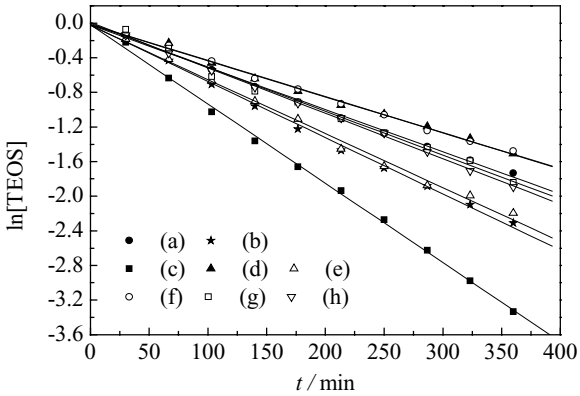

Fig. 3 The time-dependences of TEOS concentration with the molar ratio of TEOS:CH_3OH:H_2O:NH_3 at (a) 1:12.5:4:0.18 (25°C), (b) 1:12.5:4:0.18 (35°C), (c) 1:12.5:4:0.18 (45°C), (d) 1/12.5/4/0.045 (25°C), (e) 1/12.5/4/0.36 (25°C), (f) 1/12.5/2/0.18 (25°C), (g) 1/12.5/6/0.18 (25°C), (h) 1/12.5/8/0.18 (25°C). The slop of the straight line is the pseudo first-order rate constant k'_{h} of the hydrolysis reaction

Thus a linear plot of $\ln k'_{\mathrm{h}}$ vs. $\ln[\mathrm{NH_3}]$ will produce the reaction order β of NH_3 when $[H_2O]$ remains constant. This plot is shown in Fig. 4. Similarly, a linear plot of $\ln k'_{\mathrm{h}}$ vs. $\ln[H_2O]$, shown in Fig. 5, produces the reaction order γ of H_2O when $[NH_3]$ remains constant. Directly from Figs. 4 and 5, $\beta = 0.333$ and $\gamma = 0.227$ have been calculated. Applying $\ln k'_{\mathrm{h}}$ obtained from Fig. 3, β and γ in Eq. (6), k_{h1} has been calculated and listed in Table 3. Finally at 25°C the initial hydrolysis rate equation of TEOS is

$$r_{\mathrm{TEOS}} = 7.41 \times 10^{-3}[\mathrm{TEOS}][\mathrm{NH_3}]^{0.333}[\mathrm{H_2O}]^{0.227} \quad (10)$$

From Eqs. (2) and (3), the disappearance of Q_0^1 is accompanied by the appearance of Q_0^3. But the intermediate Q_0^1 is so reactive that it has little time to accumulate. After Q_0^1 content approaches its maximum, it reaches a steady state. According to the steady-state approximation [15, 16], following equation has been acquired

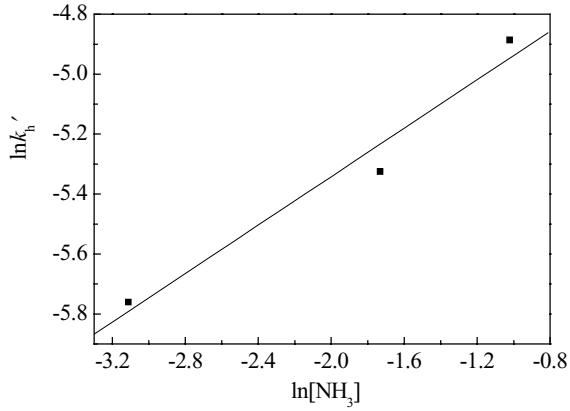

Fig. 4 The pseudo first-order rate constant k'_{h} vs. ammonium concentration for the solutions with molar ratio of TEOS:CH_3OH:H_2O:NH_3 at (a) 1:12.5:4:0.18 (25°C), (d) 1/12.0/4/0.045 (25°C), (e) 1/12.5/4/0.36 (25°C)

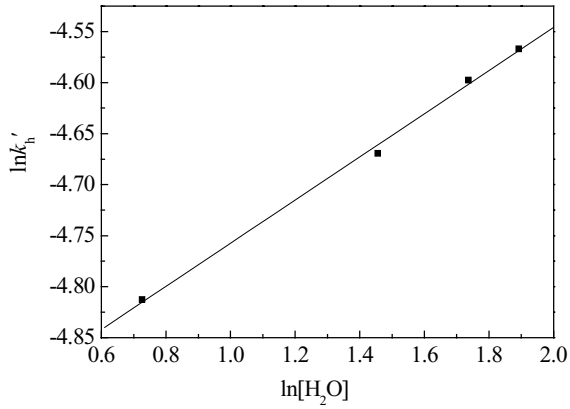

Fig. 5 The pseudo first-order rate constant k'_{h} vs. water concentration for the solutions with molar ratio of TEOS:CH_3OH:H_2O:NH_3 at (a) 1:12.5:4:0.18 (25°C), (f) 1/12.5/2/0.18 (25°C), (g) 1/12.5/6/0.18 (25°C), (h) 1/12.5/8/0.18 (25°C)

Table 3 Reaction rate constants

Sample	k'_h	k_{h1}	k_{h2}	k_c
	$\times 10^{-3}$			
(a)	4.87	7.31	42.97	151.0
(b)	6.70	10.68	83.58	313.3
(c)	9.14	13.71	106.97	488.8
(d)	2.61	7.35	52.64	170.4
(e)	6.25	7.42	45.64	158.1
(f)	4.17	7.34	48.73	163.2
(g)	5.08	7.45	54.13	162.1
(h)	5.13	7.59	56.64	145.3
Average at 25°C		7.41	50.13	158.4

The errors of k_{h1}, k_{h2} and k_c are estimated from the 5% error of integration area in NMR, and subscripts h and c indicate the hydrolysis and the condensation respectively.

$$d[Q_0^0]/dt = k_{h1}[Q_0^0]_{ss} - k_{h2}[Q_0^1]_{ss} \approx 0, \tag{11}$$

where $[Q_0^0]_{SS}$ and $[Q_0^1]_{SS}$ are the steady-state concentrations. Hence the second hydrolysis rate constant k_{h2} can be defined by

$$k_{h2} = k_{h1}[Q_0^0]_{ss}/[Q_0^1]_{ss} \tag{12}$$

The obtained k_{h2} are also listed in Table 3. From Eqs. (3) and (4), the rate constant k_c is calculated when applying the steady-state approximation to Q_0^3. The results of k_c are also summarized in Table 3.

The ^{29}Si NMR spectra of the solutions reacting at 25°C (a) and 45°C (c), are shown in Fig. 1. The temperature-dependence of rate constants can be represented by the Arrhenius equation,

$$\ln k = \ln A - E_a/RT, \tag{13}$$

where k is the rate constants of reactions (2)–(4); A is the Arrhenius factor; E_a is the activation energy of reaction (2)–(4); T is the temperature and R is the ideal gas constant (8.3145 J · mol^{-1} · K^{-1}). The plot of ln$k$ vs. $1/T$ is shown in Fig. 6 whose slope gives $-E_a/R$, and the intercept is ln$A$. So reaction activation energies and Arrhenius factors of reaction (2)–(4) are summarized in Table 4.

3.3 Determination of rate-limiting step

Seen in Table 3, k_{h1} is one order less than k_{h2}, and k_{h2} is one order less than k_c. In another word, the reaction rate

Table 4 The activation energies and Arrhenius factors

Reaction	Ea (KJ · mol^{-1})	A
(1)	24.85	169
(2)	36.09	96761
(3)	46.38	21210353

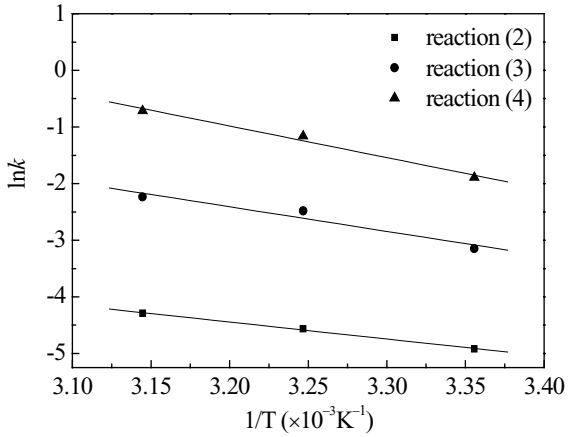

Fig. 6 Arrhenius plots of solution with TEOS:CH_3OH:H_2O:NH_3 at 1:12.5:4:0.18

is gradually increased along a sequence of $k_{h1} < k_{h2} < k_c$, which can be explained by S_N2-Si nucleophilic replacement mechanism [17, 18]. Under basic conditions, it is likely that water dissociates to produce nucleophilic hydroxyl anions in a rapid step and then the hydroxyl anion attacks the silicon atom. Iler [19] and Keefer [20] proposed an S_N2-Si mechanism in which OH^- displaces EtO^- with inversion of the silicon tetrahedron.

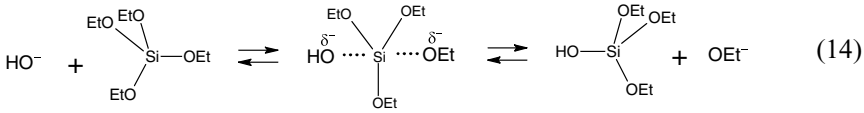

(14)

With monomer's hydrolysis proceeding, –OEt is gradually substituted for –OH. Because the electron-withdrawing capabilities of –OH is stronger than that of –OEt, the replacement of –OEt by –OH leads to more positive charge on Si atom, which benefits the further nucleophilic attack of OH^- to Si^+. So the subsequent hydrolysis occurs more quickly. At the same time, it is common that the condensation of ethoxysilanes is faster than the hydrolysis under basic conditions. From the above-mentioned standpoints, reaction (2) is the slowest one in the continuous hydrolysis and condensation, indicating that the first hydrolysis of TEOS is the rate-limiting step and the formed Q_0^1 is the key intermediate species. Our results proved quantitatively that the initial hydrolysis of TEOS was the rate-limiting step, which was consistent with the results of Lee [3], Matsoukas

[4] and Green [7], but contradicted with the viewpoints of references [5, 21].

From Fig. 1 and Table 2, no resonance signal of Q_0^2 was detected during the evolving period of TEOS. In fact, it is very difficult to observe this signal because of the fast consumption of Q_0^2. According to Green's study [7], the NMR signal of Q_0^2 can be detected only when the concentrations of water and ammonia are very low because in this case the total reaction rate is slow and the consumption of Q_0^2 is slowed down too. Therefore intermediate Q_0^2 is only a short-life transition species that will converse to Q_0^3 at once. In addition, the concentration sum of all the detectable Si species except for TEOS is 1%–8% of the total Si content in composition. The disappeared Si source mainly participates nucleation and becomes insoluble and undetectable by liquid NMR.

From Table 4, the activation energy increases from reaction (2), (3) to (4). The activation energy of reaction (2) is the lowest in those tree reactions, indicating that reaction (2) is the easiest to occur. But simultaneously reaction (2) is the slowest in those tree reactions, which seems to contradict with its activation energy. If the Arrhenius factors are taken into account, the contribution of Arrhenius factor to rate constant should be much more than that of activation energy. So reaction (2) becomes the rate-limiting step although its activation energy is less than those two reactions.

3.4 Comparison with the previous researches

From 1990s then on, many efforts have been made to correctly understand the reaction mechanism of the sol-gel process of metal alkoxides among which organic siloxane may be the simplest sol-gel precursor. However, this is not an easy work to track the true sol-gel process even its initial stage because the formation of so-called sol involves complex chemical reactions and a variation from homogeneous solution of precursor to heterogeneous colloidal suspension of particles. In the previous researches, several technologies have been employed to investigate the reaction mechanism and the subsequent particle growth mechanism, including nuclear magnetic resonance, Raman spectroscopy, gas chromatography, conductivity, infrared spectroscopy, dynamic light scattering, and small angle X-ray scattering. Although much progress has been made in this field, the precise chemical reaction kinetics is still a problem.

Reported in 1990, considering ammonia as the base catalyst and the ionization reaction of ammonia with water, Harris [6] deduced a reaction rate equation like follow:

$$d[\mathrm{TEOS}]/dt = -k_{\mathrm{H}}^{*}[\mathrm{H_2O}]^{1.5}[\mathrm{NH_3}]^{0.5}[\mathrm{TEOS}]. \quad (15)$$

The rate Eq. (15) is based on the overall hydrolysis and condensation reactions as follows:

$$\mathrm{Si(OEt)_4} + 4\mathrm{H_2O} \xrightarrow{\mathrm{OH^-}} \mathrm{Si(OH)_4} + 4\mathrm{EtOH} \quad (16)$$

$$\mathrm{Si(OH)_4} \xrightarrow{\mathrm{OH^-}} \mathrm{SiO_2} + 2\mathrm{H_2O} \quad (17)$$

However the hydrolysis of TEOS is a step-by-step process and runs nearly simultaneously with the condensation. Therefore Eq. (16) is only an ideal expression to the true reaction situation. The reaction mechanism should be more complex. In fact, the hydrolysis rate constant obtained by Harris, k_{H}^{*}, was a collective reflection of hydrolysis rates of all steps, not same as the k_{h1} obtained by us. Although Eq. (15) takes the same form as Eq. (10), the obviously different exponentials reflect the entirely different calculating base. Additionally, the condensation rate constant obtained by Harris, k_{C}^{*}, was taken by assuming that the hydrolysis and condensation of TEOS can be completely separated like Eqs. (16) and (17). So k_{H}^{*} and k_{C}^{*} were not obtained on the same level of mechanism as k_{h1}, k_{h2}, and k_{c} in this paper.

In 1997, Lee and coworker [3] reported an in-situ investigation of **S**töber reaction by ^{29}Si NMR, photon correlation spectroscopy, and conductivity. They thought that, since in an ordinary Stöber system there is only one reaction intermediate detectable by ^{29}Si NMR, an acid-base two-step catalysis to TEOS should be employed. Thus, there were eight NMR signals could be detected. But this experiment method did not reflect the true condition of Stöber reaction either. Therefore, the two-step procedure, especially employed in Lee's study, makes their results not directly comparable with the results presented in this paper. Although, they obtained a valuable conclusion that the nucleation of Stöber reaction was rate-limited by the hydrolysis of the singly hydrolyzed monomer.

The most important experimental results about this study were reported by Green and his coworker [7] in 2003. In this literature, they first confirmed that transesterification between methanol and TEOS did occur, but it was negligible compared to the production of hydrolyzed intermediates. This conclusion ensured the reliability of in-situ ^{29}Si NMR experimental results. Another important contribution was that they proved the Q_1^6 was not the hydrolysis intermediate of TEOS. Indeed, intermediate Q_1^6 wasn't detected in our all experiments either. If possible, Q_1^6 should be the condensation product of full-hydrolyzed species $\mathrm{Si(OH)_4}$, but $\mathrm{Si(OH)_4}$ is unstable in **S**töber system due to the fast condensation of Si-OH groups. Therefore, it is reasonable that Q_1^6 doesn't exist. In addition, concerning the effects of water and ammonia concentrations, they used ^{29}Si NMR to investigate the ammonia-catalyzed hydrolysis of TEOS in methanol and ethanol ($[\mathrm{TEOS}] = 0.5\,\mathrm{M}$; $[\mathrm{NH_3}] = 0.05$–$0.1\,\mathrm{M}$; and $[\mathrm{H_2O}] = 1.1$–$4.4\,\mathrm{M}$). Their research showed that the rate constant of the rate-limiting step was largely dependent on $[\mathrm{H_2O}]$ and

[NH_3]. However, a true rate constant shouldn't be dependent on the concentrations of any reactants or catalyst. In fact, their study dealt with four ^{29}Si NMR experiments in which [H_2O] and [NH_3] were set three levels respectively. Based on such few experiments, it was difficult to disclose the precise reaction rate constants. In our experiment design, all the conditions needed for extracting kinetics parameters have been taken into account. The data fluctuation of our obtained reaction rate constants was within an acceptable error range. So it is the first time to obtain the precise kinetics parameters of **S**töber reaction. Based on our experimental results, the key hydrolysis intermediate, Q_0^1, was quantitatively confirmed as well as the rate-limiting step, which was consistent with the conclusion of Green [7].

4 Conclusions

The ammonia-catalyzed hydrolysis and condensation of TEOS in methanol were investigated by in-situ liquid ^{29}Si NMR. The growth of colloidal particles was quantificationally clarified to be controlled by the initial hydrolysis of TEOS. For the first time, a whole set of rate constants of both the rate-limiting step and the non-rate-limiting steps were obtained. Besides, the reactive orders, activation energy, and the Arrhenius factors were calculated. This study proved that the rate-limiting step is the first-step hydrolysis of TEOS and Q_0^1 is the key intermediate species for the whole reaction process.

Acknowledgments The financial support from the National Key Native Science Foundation (No. 20133040) was gratefully acknowledged.

References

1. Shingo K, Ikuko Y, Noriko Y (1997) In: Dunn BS, Mackenzzie JD, Pope EJ, Schmidt HK, Yanane M (eds) Sol-Gel Optics IV, SPIE vol. 3136. The international society for optical engineering, Bellingham, Washington
2. Stöber W, Fink A, Bohn E (1968) J Colloid Interface Sci 26: 62
3. Lee K, Look JL, Harris MT, McCormick AV (1997) J Colloid Interf Sci 194:78
4. Matsoukas T, Gulari E (1988) J Colloid Interface Sci 124: 252
5. Bogush GH, Zukoski CF (1991) J Colloid Interface Sci 142: 1
6. Harris MT, Brunson RR, Byers CH (1990) J Non-Cryst Solids 121: 397
7. Green DL, Jayasundara S, Yui-Fai Lam, Harris MT (2003) J Non-Cryst Solids 315:166
8. Sadasivan S, Duber AK, Li Y, Rasmussen DH (1998) J Sol-Gel Sci Tech 5:12
9. Harris RK, Kimber BJ (1974) J Organometal Chem 70:43
10. Bailey JK, McCartney ML (1992) Colloids Surf 151:63
11. Assink RA, Kay BD (1991) Ann Rev Mater Sci 21:491
12. Sugahara Y, Okada S, Kuroda K, Kato C (1992) J Non-Cryst Solids 139:25
13. Brinker CJ, Scherer GW (1990) Sol-gel science: the physics and chemistry of sol-gel processing. Academic Press, San Diego
14. Fyfe CA, Aroca PP (1997) J Phys Chem B 101:9504
15. Volk L, Richardson W (1977) J Chem Educ 54:95
16. David Cater E (1983) J Chem Educ 60:109
17. Parker AJ (1967) Adv Phys Org Chem 5:173
18. Parker AJ (1969) Chem Rev 1:69
19. Iler RK (1979) The chemistry of silica. Wiley, New York
20. Keefer KD (1984) In: Brinker CJ, Clark DE Ulrich DR (eds) Better ceramics through chemistry. North-Holland, New York, p 15
21. Boukari H, Long GG, Harris MT (2000) J Colloid Interf Sci 229:129